Differential and enhanced response to climate forcing in diarrheal disease due to rotavirus across a megacity of the developing world

Pamela P. Martinez[a], Aaron A. King[b,c], Mohammad Yunus[d], A. S. G. Faruque[d], and Mercedes Pascual[a,e,1]

[a]Department of Ecology and Evolution, University of Chicago, Chicago, IL 60637; [b]Department of Ecology and Evolutionary Biology, University of Michigan, Ann Arbor, MI 48109; [c]Department of Mathematics, University of Michigan, Ann Arbor, MI 48109; [d]International Centre for Diarrheal Disease Research, Dhaka 1000, Bangladesh; and [e]Santa Fe Institute, Santa Fe, NM 87501

Edited by Burton H. Singer, University of Florida, Gainesville, FL, and approved February 24, 2016 (received for review September 26, 2015)

The role of climate forcing in the population dynamics of infectious diseases has typically been revealed via retrospective analyses of incidence records aggregated across space and, in particular, over whole cities. Here, we focus on the transmission dynamics of rotavirus, the main diarrheal disease in infants and young children, within the megacity of Dhaka, Bangladesh. We identify two zones, the densely urbanized core and the more rural periphery, that respond differentially to flooding. Moreover, disease seasonality differs substantially between these regions, spanning variation comparable to the variation from tropical to temperate regions. By combining process-based models with an extensive disease surveillance record, we show that the response to climate forcing is mainly seasonal in the core, where a more endemic transmission resulting from an asymptomatic reservoir facilitates the response to the monsoons. The force of infection in this monsoon peak can be an order of magnitude larger than the force of infection in the more epidemic periphery, which exhibits little or no post-monsoon outbreak in a pattern typical of nearby rural areas. A typically smaller peak during the monsoon season nevertheless shows sensitivity to interannual variability in flooding. High human density in the core is one explanation for enhanced transmission during troughs and an associated seasonal monsoon response in this diarrheal disease, which unlike cholera, has not been widely viewed as climate-sensitive. Spatial demographic, socioeconomic, and environmental heterogeneity can create reservoirs of infection and enhance the sensitivity of disease systems to climate forcing, especially in the populated cities of the developing world.

monsoon flooding | diarrheal disease | rotavirus transmission | epidemiological model | urban health

Many infectious diseases, especially those infectious diseases that are water-borne and vector-borne, have been shown to exhibit significant interannual variability in the size of seasonal outbreaks (e.g., 1–6). Identification of climate factors shaping interannual and seasonal variability is prerequisite to an understanding of the basic transmission biology of these environmentally driven diseases, and of their response to climate change. The impact of climate factors on the population dynamics of infectious diseases has typically been addressed at large spatial scales by aggregating surveillance data over whole countries, regions, and cities (e.g., 3, 4, 6–8). Global climate drivers, such as the El Niño Southern Oscillation (ENSO), are expected to operate over large spatial scales, synchronizing fluctuations of disease incidence across space [i.e., the Moran effect in population dynamics (9, 10)]. A recent study has shown, however, that the spatiotemporal dynamics of cholera in Dhaka, Bangladesh, are not homogeneous at intra-urban scales (11). Two regions or clusters were identified, corresponding, respectively, to the highly populated core and the more rural periphery. The urban core was shown to be more climate-sensitive, acting to propagate climate perturbations in cholera infection risk to the rest of the city. Our study addresses whether such spatial heterogeneity is also visible in the response to climate forcing at seasonal and interannual time scales in another major diarrheal infection, rotavirus. Because, unlike cholera, rotavirus does not appear to possess an environmental transmission pathway, it has not been viewed as a climate-sensitive infection. Here, we examine the role of the monsoons, and particularly flooding, in modulating the transmission of rotavirus. We inquire into whether such an effect might vary across local scales within a large urban environment.

Rotavirus is the most common cause of diarrhea among infants and young children worldwide, responsible for 40% of childhood gastroenteritis hospitalizations and 37% of diarrhea-related deaths in children younger than 5 y (12, 13). This disease was recently reported to be the second most commonly isolated pathogen after *Vibrio cholerae* among adults attending urban and rural treatment facilities in Bangladesh (14). Rotavirus is transmitted primarily via the fecal-oral route, and two main seasonal patterns have been described. In temperate regions, incidence tends to peak during winter months (15–20). In the tropics, incidence exhibits less pronounced seasonal variation (16, 21), with year-round incidence and peaks during summer or fall following monsoon rains, as in Bangladesh (22, 23). Despite these contrasting patterns, few correlational studies have statistically associated environmental variables with rotavirus incidence (24, 25). We focus here on the monsoon season, and on flooding in particular, which is both a major environmental disturbance in Bangladesh and one of the more prominent local manifestations

Significance

Rotavirus is the most common cause of diarrhea among infants and children worldwide, and is still responsible for over 400,000 deaths per year, affecting mainly developing countries. This study investigates its transmission dynamics and their response to climate forcing, specifically flooding, in the megacity of Dhaka, Bangladesh, with an extensive surveillance record that spans over two decades and is spatially resolved. With a transmission model informed by these data, we show that consideration of different parts of the city, core and periphery, is critical to uncover important differences in seasonal outbreaks and in the effect of the monsoons. Infectious diseases not typically considered climate-sensitive can become so under demographic and environmental conditions of large urban centers of the developing world.

Author contributions: P.P.M., A.A.K., and M.P. designed research; P.P.M. performed research; P.P.M. analyzed data; P.P.M., A.A.K., M.Y., A.S.G.F., and M.P. wrote the paper; and M.Y. and A.S.G.F. provided data and knowledge on the system.

The authors declare no conflict of interest.

This article is a PNAS Direct Submission.

Freely available online through the PNAS open access option.

[1]To whom correspondence should be addressed. Email: pascualmm@uchicago.edu.

This article contains supporting information online at www.pnas.org/lookup/suppl/doi:10.1073/pnas.1518977113/-/DCSupplemental.

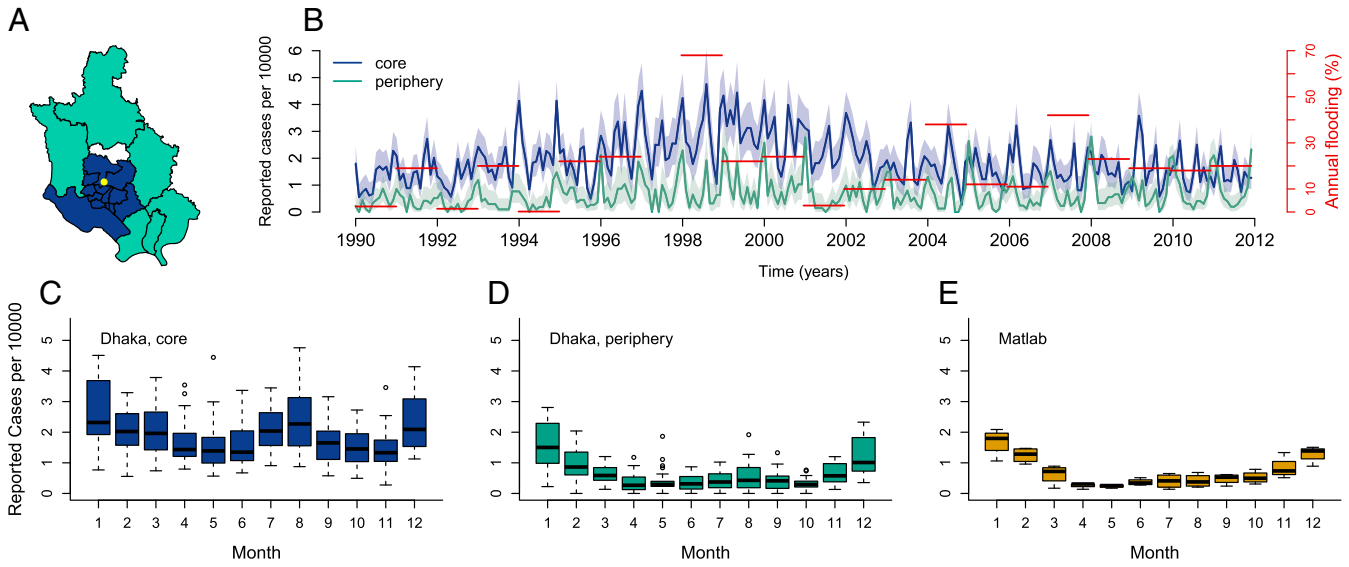

Fig. 1. Data. (*A*) Administrative subdivisions or thanas of Dhaka are divided into two groups: the core region (blue) and the periphery region (cyan), according to the grouping proposed by Reiner et al. (11). The thana in white was excluded from the analyses because of a lack of data before 2001, when it was created. The yellow dot indicates the location of the Dhaka Hospital. (*B*) Monthly cases of rotavirus from 1990 to 2011 aggregated by region and normalized by population size and annual flooding index (in red); the 95% confidence intervals of a binomial distribution test are shaded in light colors. (*C*–*E*) Box plot of the normalized rotavirus cases by month per region. Matlab is a rural area of Bangladesh located 55 km southeast of Dhaka.

of the ENSO in this region (26). Specifically, we implement stochastic transmission models to explore the effects of climate forcing within and between years, and across regions of the city. More specifically, they allow us to estimate and compare seasonal transmission intensity in the core and periphery of the city.

Our analyses show that the risk of rotavirus is far higher within the urban core, and aggregation of cases reveals distinct seasonal patterns in the core and periphery, with two peaks per year in the former (in the winter and monsoon seasons) and a single winter peak, with the second one usually absent, in the latter. Pronounced differences are further identified in the force of infection throughout the year and in its response to the monsoons, with distinct effects at the seasonal and interannual time scales for the core and periphery of the city, respectively. These findings underscore the importance of spatial heterogeneity when addressing the role of climate forcing in urban environments. An infection that is not typically considered climate-sensitive can be seen to be so within the highly populated core of the city. We discuss implications for the sensitivity of infectious diseases to changes in climate in the context of the accelerating growth of cities in decades to come.

Results

The aggregation of the 22 y of data by core and periphery (Fig. 1*A*) reveals that the incidence rate in the core is almost threefold the incidence rate in the periphery (Fig. 1*B*). The two zones display distinct, hitherto unremarked, patterns of seasonality, which are also representative of variation at the thana level (Fig. S1). Specifically, rotavirus cases in the core exhibit a temporal pattern similar to the pattern described previously for tropical countries, with one peak during winter months and another during the monsoon season (Fig. 1*C*). The average number of reported cases cumulating from June to September for the monsoon season is comparable to the number of reported cases obtained from November to February for the winter season (6% smaller). However, the second peak in cases is less pronounced in the periphery, and less than half the size of the winter peak (57% smaller; Fig. 1*D*). A similar seasonal pattern is found in Matlab, a rural area 55 km southeast of Dhaka (Fig. 1*E*). These seasonal patterns suggest important differences in disease transmission within the city. In terms of climate fluctuations, severity of flooding shows year-to-year variation, with the most severe floods recorded for the years 1998, 2004, and 2007 (Fig. 1*B*).

Using a stochastic transmission model (Fig. 2), we tested two different hypotheses. The best model includes flooding as a covariate and performs significantly better than the model without this interannual effect, based on a likelihood ratio test

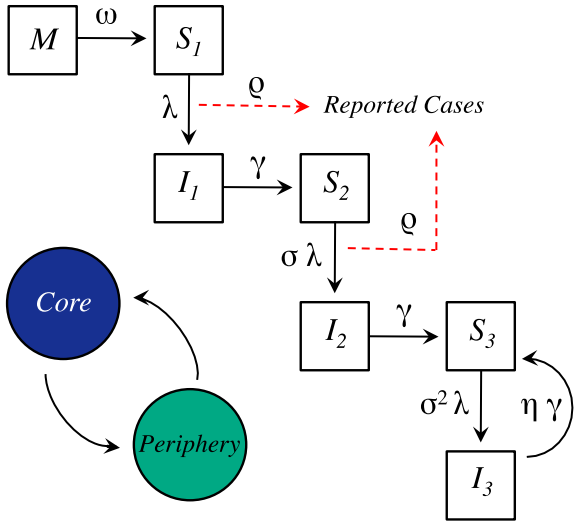

Fig. 2. Diagram of the transmission model of rotavirus. The arrows indicate rates of flow among compartments. Each population, for the core and periphery, respectively, is divided into the following classes: newborn (*M*), susceptible (S_1, S_2, S_3), and infected (I_1, I_2, I_3). The three levels of susceptible and infected individuals are meant to represent the recurrent exposure of individuals to the pathogen, as they acquire increasing protection and eventually become asymptomatic (after the second infection). The effect of movement between populations is incorporated within the force of infection (Eq. **2**).

Table 1. Likelihood-based comparison of the different models

Model	Log-likelihood	SE	No. of parameters	AIC	Likelihood ratio test
With flooding effect	−1577.6	0.33	25	3205.2	
Without flooding effect	−1582.2	0.35	23	3210.4	$P = 0.01$

($P = 0.01$; Table 1). Fig. 3 illustrates simulations of the monthly cases from estimated initial conditions from 1990 to 2012 for the best model compared with the observed cases. The best-fitting model captures the interannual variation (Fig. 3*A*) and the main seasonal pattern of the reported cases in both regions (Fig. 3*B*). Moreover, this model reveals a striking difference in the force of infection (the instantaneous infection risk to each susceptible individual) between both regions, with larger values in the core than in the periphery (Fig. 4 *A* and *B*). This difference is of an order of magnitude for the monsoon season, suggesting a higher intensity of transmission during this period. Interestingly, the estimated seasonality of the force of infection for the core of the city is similar to the estimated seasonality of the force of infection for cases in tropical countries, with one peak during winter and another during the monsoon season, and sustained transmission throughout the year. In contrast, the force of infection in the periphery shows one dominant peak during winter and a typically much weaker peak during the monsoon season, with a more epidemic pattern with deeper troughs between those seasons. The second peak is apparent here only in years with large flooding events (Fig. S2): In the periphery, the transmission rate during the monsoon season has a much lower average, yet a more pronounced interannual response to large floods (Fig. 4*C*).

The maximum likelihood estimates of the parameters reveal additional features of the dynamics (Table 2 and Figs. S3 and S4): The coupling between the core and periphery appears weak ($\alpha_c = 0.96$ and $\alpha_p = 0.87$), maternal immunity of newborn individuals ($1/\omega$) wanes rapidly, the duration of infection ($1/\gamma$) is between 7 and 15 d, and individuals in the I_3 class have an infection that is long-lasting ($1/\eta$, about 16-fold longer). As we discuss below, we interpret the value of this duration as indicating the presence of a transmission reservoir.

Finally, an alternative explanation for the higher overall number of cases in the core than in the periphery, and for their differential seasonality, might be that access to the hospital, which is located in the former region (Fig. 1), is limited and especially impaired during the monsoons. Differences in hospital attendance rather than in the force of infection would explain the empirical patterns. To test this alternative hypothesis, an additional model was considered in which the transmission rate is the same for both regions but their reporting rate differs. Four reporting rates are estimated to allow for different values outside and inside the monsoon season (June through September) for the core and periphery, respectively. The log-likelihood of this model was 29 units lower than our best model [log-likelihood = −1,606.9 and Akaike information criterion (AIC) = 3,256 vs. log-likelihood = −1,577.6 and AIC = 3,205]. Additional arguments against this alternative explanation are presented below.

Discussion

Consideration of two different parts of the city, a densely populated core and a more rural periphery, appears essential to understand seasonal and interannual variation of this major diarrheal infection in response to climate forcing by the monsoons. In particular, our analysis reveals pronounced spatial heterogeneity in both the overall magnitude and the temporal pattern of disease risk within the city. Our results provide evidence that these two regions respond differentially to climate forcing, consistent with previous findings for cholera in the same region (11). The contrasting seasonal patterns described here within the city are consistent with the findings of a recent metaanalysis on rotavirus seasonality proposing that climatic conditions and the degree of country development are better predictors than latitude or geographic location per se (21, 27). The cholera study (11) also suggested that this level of aggregation (core and periphery) is congruent with spatial variation in socioeconomic conditions, including population density (Fig. S5). These factors may act to modulate the effect of climate variables at local spatial scales by enhancing contact and population susceptibility. It is interesting to note that the climate sensitivity of cholera has been traditionally explained with reference to the residence of its etiological agent, the bacterium *V. cholerae*, in aquatic

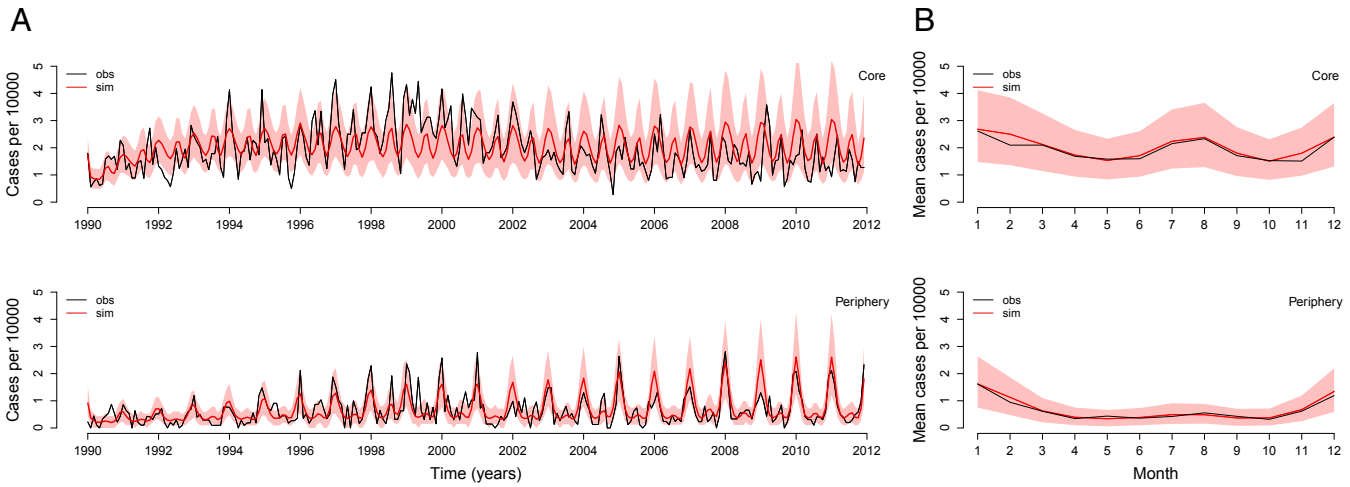

Fig. 3. Comparison of simulated cases with those cases reported for the core and periphery of Dhaka. Time series (*A*) and seasonal pattern (*B*) for the observed cases (obs; black) and the mean of 1,000 model simulations (sim; red). The 10% and 90% percentiles of the simulated data are shaded in light red. The model simulations are not next step predictions, but numerical simulations of the model forward for the whole time period of the study starting with estimated initial conditions.

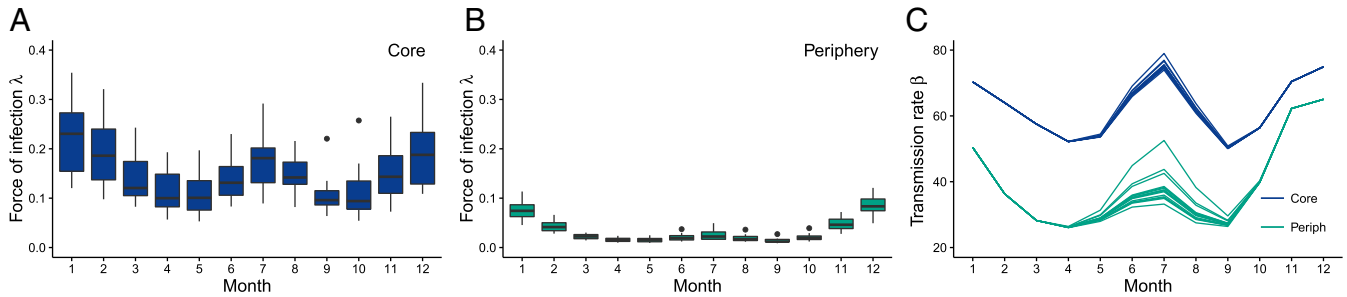

Fig. 4. Force of infection and transmission rate from one simulation for the period 1997–2011. (*A* and *B*) Box plot of the force of infection by month per region. The force of infection is defined as the per capita rate at which susceptible individuals become infected. (*C*) Transmission rate by month per region. The maximum peak value relative to the mean for the monsoon season equals 1.05 and 1.36 for the core and periphery (Periph), respectively. Corresponding estimates of R_0 are provided in *Supporting Information*.

environments independent of the human host (28). The fact that rotavirus displays climate sensitivity too, in the absence of such an environmental reservoir, suggests that the causal links in the climate–disease connection are not strictly dependent on specific ecological mechanisms related to transmission pathways (29). A similar association with sea surface temperatures in the Pacific for cholera and shigellosis in Bangladesh suggested that the ENSO acts mainly via the modulation of secondary transmission in these diarrheal diseases (e.g., by increasing exposure to contaminated water as well as person-to-person contact) (30).

In addition to socioeconomic and demographic factors, the two regions of the city might more directly differ in susceptibility to flooding itself. Flooding risk and extent appear heterogeneous throughout the city (31), but in a way that is not consistent with this explanation. Moreover, during extreme floods, such as the floods of 1998, more than 50% of the city's area can be inundated (32).

Our results suggest the presence of a transmission reservoir that maintains transmission between seasons and primes the seasonal response of the system to the monsoons. The existence of such a reservoir is implied by the long duration of infection in the most immune class (I_3), whose individuals are asymptomatic in our model. The more endemic epidemiological pattern of the core region is generated in the model via this reservoir conjoined with high transmission rates. In the core, the monsoon season peak is highly regular, and the relatively small interannual variability in this peak suggests rapid saturation of the transmission system during the season. In the periphery, by contrast, low transmission rates lead to a more epidemic pattern of dynamics (deeper troughs), where the magnitude of the second peak is limited by the rate of transmission during the monsoon season, which varies substantially from year to year. Thus, the degree of interannual and seasonal sensitivity to climate would vary across a transmission gradient, as documented for climate-sensitive diseases, such as malaria, via comparisons of disease dynamics in endemic vs. fringe regions (33, 34), and within an urban landscape here.

The validity of our conclusions vis-à-vis transmission presupposes that the patterns we see in the incidences are not merely due to differential hospital-seeking behavior in the two parts of the city. Three pieces of evidence suggest that this differential reporting rate is not the case. First, the similarity in the seasonal pattern and overall incidence rate between the periphery of Dhaka and the rural area of Matlab, 40 km southeast and the site of an intensive and well-established surveillance system, supports that the observed differences are not merely an artifact of biases in hospital attendance rates. Second, rotavirus rates do not track seasonal rates in hospital attendance rates (e.g., the former decline in the periphery in March, April, and May when values of the latter increase; Fig. S6). Hospital-seeking behavior is driven by a variety of diarrheal infections, particularly by cholera during those months. Finally, we formulated a model specifically allowing for differential reporting rates between the regions and seasons; this model is rejected by the model selection criteria ($P < 0.0001$).

Relationships between force of infection, reinfection frequency, and severity of disease shape the age distribution of cases. Under similar case age distributions across the city, which we find for Dhaka (Fig. S7), the estimated higher force of infection in the core implies that children there also experience more frequent bouts of infection. Pitzer et al. (35) fitted a model similar to ours to age-distribution data, under the assumption of stationarity. We have focused here instead on the dynamic behavior of the system and fitted the model to time series of incidence, ignoring age structure. The fact that these contrasting approaches lead to models that differ in several particulars, including the basic reproduction number, R_0, emphasizes the remaining uncertainties in model structure and parameter values. To resolve these issues, it will be useful to fit rotavirus transmission models to time series of age-specific incidence. Such an effort should further elucidate rotavirus epidemiology and, in particular, the relationship between age structure and force of infection in models with a more complex structure than the well-understood susceptible–infected–recovered (SIR) formulation.

The coupling of the population dynamics of the virus between the two regions of the city is weak in our best model. This result could be further investigated in the future with explicit spatiotemporal information on human movement within the city based on mobile phone data and census data, because these methods continue to develop and have already contributed to a better spatial understanding of transmission in other infectious diseases (36–40). Further research of relevance to early warnings would also benefit from better data on flooding with higher spatiotemporal resolution, more congruent with the spatial scale of the city and the temporal scale of the seasonal transmission dynamics. A finer resolution would allow the explicit consideration

Table 2. Parameter estimates and confidence intervals

Description	Value	Confidence interval
$1/\mu$ Average lifespan, y	50	Fixed
$1/\gamma$ Duration of infection, d	10	7–15
$1/\omega$ Duration of maternal immunity, d	1	0–110
ρ Reporting rate (10^{-3})	2.3	1.8–3.6
α_c Coupling core	0.96	0.90–0.98
α_p Coupling periphery	0.87	0.31–1.00
σ Susceptibility reduction	0.19	0.12–0.24
η Additional duration of infection	0.06	0.04–0.09

of flooding as a seasonal driver. In addition, investigation of seasonal forecasts from hydrological models is warranted. Finally, other model structures should be investigated to examine the nature of the reservoir better and to take into account existing serotype variation within the virus population.

To conclude, our results underscore the importance of considering the spatial heterogeneity of large urban environments when analyzing climate-driven transmission dynamics. Urban heterogeneity can enhance sensitivity of transmission dynamics to climate factors via demographic and socioeconomic conditions, even in infectious diseases that are not necessarily recognized as climate-sensitive to begin with. These conditions can facilitate the persistence of reservoirs of infection and, in so doing, facilitate responses to anomalous climate events and seasonal environmental variation, especially in the populated cities of the developing world and in the future under climate change.

Materials and Methods

Data. Records of rotavirus cases confirmed by ELISA were obtained from the Dhaka Hospital, through the ongoing and long-term surveillance program of the International Centre for Diarrheal Disease Research, Bangladesh (ICDDR,B). A sample was taken for every 25th patient who visited the hospital from 1990 to 1995, and for every 50th patient from 1996 to 2011. These samples were extrapolated to correct for the frequency of sampling and to produce a consistent time series across time. The cases were aggregated by month per administrative subdivision or thana. The population for each thana was exponentially interpolated from the decadal censuses (1981, 1991, and 2001) to generate the monthly values. The cases were then aggregated for the two different parts of the city as proposed by Reiner et al. (11) (core and periphery; Fig. 1*A*). The monthly data for Matlab of rotavirus cases for the period 2010–2013 were obtained from the Matlab Hospital. The flooding data consist of the annual percentage of country area flooded, provided by the Annual Flood Report of the Flood Forecasting and Warning Centre, Bangladesh. We drive the model with the flooding anomaly F (the flooding index with its mean value subtracted). For data access, coauthors from the ICDDR,B should be contacted and data access would be guided by the data-sharing policy of the ICDDR,B.

Transmission Model. To describe the population dynamics of the disease within a region, we adapted the model proposed by Pitzer et al. (41) and coupled transmission between regions (Fig. 2). Newborns enter the M_i class, where they are protected from infection by maternal Abs. This maternally acquired immunity wanes at rate ω as individuals are transferred to the first susceptible class S_{1i}. Because individuals may be infected multiple times during their lifetime (42), gaining immunity by repeated exposure, we considered a structure with multiple classes of infected (I_1, I_2, I_3) and susceptible (S_1, S_2, S_3) individuals. Although the recovery class is not included, the model takes into account partial immunity from previous exposure to the pathogen through a reduction in susceptibility following the first infection (σ). Other epidemiological parameters are described in Table 2. The set of stochastic differential equations is given by the following:

$$\begin{aligned}
\frac{dM_i}{dt} &= \left(\mu P_i + \frac{dP_i}{dt}\right) - \omega M_i - \mu M_i \\
\frac{dS_{1i}}{dt} &= \omega M_i - \lambda_i S_{1i} - \mu S_{1i} \\
\frac{dI_{1i}}{dt} &= \lambda_i S_{1i} - \gamma I_{1i} - \mu I_{1i} \\
\frac{dS_{2i}}{dt} &= \gamma I_{1i} - \lambda_i \sigma S_{2i} - \mu S_{2i} \\
\frac{dI_{2i}}{dt} &= \lambda_i \sigma S_{2i} - \gamma I_{2i} - \mu I_{2i} \\
\frac{dS_{3i}}{dt} &= \gamma I_{2i} + \eta\gamma I_{3i} - \lambda_i \sigma^2 S_{3i} - \mu S_{3i} \\
\frac{dI_{3i}}{dt} &= \lambda_i \sigma^2 S_{3i} - \eta\gamma I_{3i} - \mu I_{3i}.
\end{aligned} \qquad [1]$$

P_i represents population size, and the flow of newborns combined with the death rate of each class results in population numbers equal to the population numbers observed for the growth of the city. Furthermore, the force of infection (or rate of transmission per susceptible individual) of each population is given by the following expression:

$$\lambda_i = \beta_i \left[\alpha_i \frac{(I_{1i} + I_{2i} + I_{3i})}{P_i} + (1 - \alpha_j) \frac{(I_{1j} + I_{2j} + I_{3j})}{P_i} \right], \qquad [2]$$

where β_i is the transmission rate for population i and $(1 - \alpha_i)$ refers to the movement rate of infected individuals from region i to j, and vice versa. The transmission rate is, in turn, given by the following:

$$\beta_i = \exp\left[\sum_{k=1}^{6} b_{ki} s_k + b_{fi} s_4 F \right] \left[\frac{d\Gamma}{dt} \right], \qquad [3]$$

and includes three components: (*i*) periodic functions of time to incorporate the seasonality through six splines s_k (Fig. S8) and their respective coefficients b_k; (*ii*) the interannual effect of flooding (F); and (*iii*) environmental noise through a Gamma distribution Γ, which represents stochastic variability absent in the climate covariate [details are provided in the study by Laneri et al. (6)]. We note that the effect of climate forcing by the monsoons enters at two different time scales, seasonal and interannual, in this expression. The seasonal effect is represented implicitly by the coefficient b_{ki}, specifically by b_{4i}, because the fourth spline (s_4) peaks during the monsoon months (Fig. S8); we therefore interpret the seasonal component quantified by this term as the average influence of the monsoon, which might include effects of humidity and temperature, and not necessarily or uniquely the effects of flooding. Additional variability is introduced across years through explicit consideration of an interannual effect of flooding (F), which, as a major manifestation of the monsoons, is also localized during those same months by its dependency on s_4 and multiplicatively modulates this seasonal component (Eq. **3**).

We assume that reported cases are sampled from a negative binomial distribution, allowing for measurement noise: $\text{cases}_t \sim \text{NegBin}(\rho C_i, k_i)$ with mean ρC_i and overdispersion k_i. The reporting rate is ρ, and C_i represents the symptomatic infected individuals for population i coming from the sum of the individuals entering in class I_1 and I_2 at time t (Fig. 2). Two additional models are described in *Supporting Information*. The first one adds an additional parameter to the above model to allow for differential infectiousness of the infected classes. The second one allows us to investigate the hypothesis that the differences between the core and periphery arise from biases in hospital attendance for the core and periphery.

Parameter Estimation and Model Selection. The estimation of both parameters and initial conditions for all state variables was carried out with an iterated filtering algorithm (MIF, for maximum likelihood iterated filtering) implemented in the R package "pomp" [partially observed Markov processes (43–45)]. This algorithm maximizes the likelihood and allows for the inclusion of both measurement and process noise, in addition to hidden variables, which is a typical limitation of surveillance records that provide a time series for a single observed variable per region. The initial search of parameter space was performed with a grid of 10,000 random parameter combinations, and the output of this search was used as the initial conditions of a more local search. We repeated this process until the maximum likelihood value was stationary. All parameters were estimated, except for μ, which was based on the average lifespan of an individual.

Likelihood-based criteria were used for model selection, including a likelihood ratio test because the models are nested and the AIC, which penalizes the likelihood based on the number of parameters, thus taking into account model complexity.

ACKNOWLEDGMENTS. We thank two anonymous referees for their insightful comments. This work was completed in part with resources provided by the University of Chicago Research Computing Center. This research was partially supported by the National Oceanic and Atmospheric Administration (Grant F020704). The case data used in this paper were collected with the support of the ICDDR,B and its donors, who provide unrestricted support to the ICDDR,B for its operation and research. Current donors providing unrestricted support include the Government of the People's Republic of Bangladesh; the Department of Foreign Affairs, Trade, and Development Canada; the Swedish International Development Cooperation Agency; and the Department for International Development (UK Aid). We thank these donors for their support and commitment to the ICDDR,B's research efforts. A.A.K. was supported by the Research and Policy in Infectious Disease Dynamics program of the Science and Technology Directorate, US Department of Homeland Security; by the Fogarty International Center, US NIH; and also by research grants from the NIH (Grant 1R01AI101155) and Models of Infectious Disease Agent Study (MIDAS), National Institute of General Medical Sciences (Grant U54-GM111274).

1. Pascual M, Rodó X, Ellner SP, Colwell R, Bouma MJ (2000) Cholera dynamics and El Niño-Southern Oscillation. *Science* 289(5485):1766–1769.
2. Zhou G, Minakawa N, Githeko AK, Yan G (2004) Association between climate variability and malaria epidemics in the East African highlands. *Proc Natl Acad Sci USA* 101(8):2375–2380.
3. Cazelles B, Chavez M, McMichael AJ, Hales S (2005) Nonstationary influence of El Niño on the synchronous dengue epidemics in Thailand. *PLoS Med* 2(4):e106.
4. Koelle K, Rodó X, Pascual M, Yunus M, Mostafa G (2005) Refractory periods and climate forcing in cholera dynamics. *Nature* 436(7051):696–700.
5. Nagao Y, Koelle K (2008) Decreases in dengue transmission may act to increase the incidence of dengue hemorrhagic fever. *Proc Natl Acad Sci USA* 105(6):2238–2243.
6. Laneri K, et al. (2010) Forcing versus feedback: Epidemic malaria and monsoon rains in northwest India. *PLOS Comput Biol* 6(9):e1000898.
7. Hoshen MB, Morse AP (2004) A weather-driven model of malaria transmission. *Malar J* 3(1):32–46.
8. Sultan B, Labadi K, Guégan JF, Janicot S (2005) Climate drives the meningitis epidemics onset in west Africa. *PLoS Med* 2(1):e6.
9. Moran PAP (1953) The statistical analysis of the Canadian lynx cycle. *Aust J Zool* 1(3):291–298.
10. Hudson PJ, Cattadori IM (1999) The Moran effect: A cause of population synchrony. *Trends Ecol Evol* 14(1):1–2.
11. Reiner RC, Jr, et al. (2012) Highly localized sensitivity to climate forcing drives endemic cholera in a megacity. *Proc Natl Acad Sci USA* 109(6):2033–2036.
12. Parashar UD, Hummelman EG, Bresee JS, Miller MA, Glass RI (2003) Global illness and deaths caused by rotavirus disease in children. *Emerg Infect Dis* 9(5):565–572.
13. Tate JE, et al.; WHO-coordinated Global Rotavirus Surveillance Network (2012) 2008 estimate of worldwide rotavirus-associated mortality in children younger than 5 years before the introduction of universal rotavirus vaccination programmes: A systematic review and meta-analysis. *Lancet Infect Dis* 12(2):136–141.
14. Ferdous F, et al. (2015) Aetiologies of diarrhoea in adults from urban and rural treatment facilities in Bangladesh. *Epidemiol Infect* 143(7):1377–1387.
15. Konno T, et al. (1983) Influence of temperature and relative humidity on human rotavirus infection in Japan. *J Infect Dis* 147(1):125–128.
16. Cook SM, Glass RI, LeBaron CW, Ho MS (1990) Global seasonality of rotavirus infections. *Bull World Health Organ* 68(2):171–177.
17. Purohit SG, Kelkar SD, Simha V (1998) Time series analysis of patients with rotavirus diarrhoea in Pune, India. *J Diarrhoeal Dis Res* 16(2):74–83.
18. Bresee J, et al.; Asian Rotavirus Surveillance Network (2004) First report from the Asian Rotavirus Surveillance Network. *Emerg Infect Dis* 10(6):988–995.
19. Nakagomi T, et al. (2005) Incidence and burden of rotavirus gastroenteritis in Japan, as estimated from a prospective sentinel hospital study. *J Infect Dis* 192(Suppl 1): S106–S110.
20. D'Souza RM, Hall G, Becker NG (2008) Climatic factors associated with hospitalizations for rotavirus diarrhoea in children under 5 years of age. *Epidemiol Infect* 136(1): 56–64.
21. Levy K, Hubbard AE, Eisenberg JNS (2009) Seasonality of rotavirus disease in the tropics: A systematic review and meta-analysis. *Int J Epidemiol* 38(6):1487–1496.
22. Hieber JP, Shelton S, Nelson JD, Leon J, Mohs E (1978) Comparison of human rotavirus disease in tropical and temperate settings. *Am J Dis Child* 132(9):853–858.
23. Stoll BJ, et al. (1982) Surveillance of patients attending a diarrhoeal disease hospital in Bangladesh. *Br Med J (Clin Res Ed)* 285(6349):1185–1188.
24. Rahman M, et al. (2007) Prevalence of G2P[4] and G12P[6] rotavirus, Bangladesh. *Emerg Infect Dis* 13(1):18–24.
25. Hashizume M, et al. (2008) Rotavirus infections and climate variability in Dhaka, Bangladesh: A time-series analysis. *Epidemiol Infect* 136(9):1281–1289.
26. Cash BAX, Rodó JL, Kinter III (2008) Links between tropical Pacific SST and cholera incidence in Bangladesh: Role of the eastern and central tropical Pacific. *J Clim* 21: 4647–4663.
27. Patel MM, et al. (2013) Global seasonality of rotavirus disease. *Pediatr Infect Dis J* 32(4):e134–e147.
28. Colwell RR (1996) Global climate and infectious disease: Tthe cholera paradigm. *Science* 274(5295):2025–2031.
29. Lipp EK, Huq A, Colwell RR (2002) Effects of global climate on infectious disease: The cholera model. *Clin Microbiol Rev* 15(4):757–770.
30. Cash BA, et al. (2014) Cholera and shigellosis: Different epidemiology but similar responses to climate variability. *PLoS One* 9(9):e107223.
31. Dewan A, Corner R (2014) *Dhaka Megacity Geospatial Perspectives on Urbanisation, Environment and Health* (Springer, Dordrecht).
32. Faisal IM, Kabir MR, Nishat A (2003) The disastrous flood of 1998 and long-term mitigation strategies for Dhaka City. *Nat Hazards (Dordr)* 28:85–99.
33. Laneri K, et al. (2015) Dynamical malaria models reveal how immunity buffers effect of climate variability. *Proc Natl Acad Sci USA* 112(28):8786–8791.
34. Pascual M (2015) Climate and Population Immunity in Malaria Dynamics: Harnessing Information from Endemicity Gradients. *Trends Parasitol* 31(11):532–534.
35. Pitzer VE, et al. (2011) Influence of birth rates and transmission rates on the global seasonality of rotavirus incidence. *Journal of the Royal Society Interface* 8(64):1584–1593.
36. Wesolowski A, et al. (2012) Quantifying the impact of human mobility on malaria. *Science* 338(6104):267–270.
37. Buckee CO, Wesolowski A, Eagle NN, Hansen E, Snow RW (2013) Mobile phones and malaria: Modeling human and parasite travel. *Travel Med Infect Dis* 11(1):15–22.
38. Dalziel BD, Pourbohloul B, Ellner SP (2013) Human mobility patterns predict divergent epidemic dynamics among cities. *Proc Biol Sci* 280(1766):20130763.
39. Richardson DB, et al. (2013) Medicine. Spatial turn in health research. *Science* 339(6126):1390–1392.
40. Wesolowski A, Eagle N, Noor AM, Snow RW, Buckee CO (2013) The impact of biases in mobile phone ownership on estimates of human mobility. *J R Soc Interface* 10(81): 20120986.
41. Pitzer VE, et al. (2009) Demographic variability, vaccination, and the spatiotemporal dynamics of rotavirus epidemics. *Science* 325(5938):290–294.
42. Velázquez FR, et al. (1996) Rotavirus infections in infants as protection against subsequent infections. *N Engl J Med* 335(14):1022–1028.
43. Ionides EL, Bretó C, King AA (2006) Inference for nonlinear dynamical systems. *Proc Natl Acad Sci USA* 103(49):18438–18443.
44. King AA, et al. (2015) pomp: Statistical Inference for Partially Observed Markov Processes (R package, version 1.0.0.0). Available at pomp.r-forge.r-project.org. Accessed May 1, 2015.
45. King AA, Nguyen D, Ionides EL (2015) Statistical inference for partially observed Markov processes via the R Package pomp. *J Stat Softw*, in press.